3D modeling and volume measurement of bulk grains stored in large warehouses using bi-temporal multi-site terrestrial laser scanning data

Xingbo Hu,[1] Tian Xia,[1] Leidong Yang,[2] Fangming Wu,[2] Ying Fan,[3] Yinghong Tian[1]

[1]School of Communication and Electronic Engineering, East China Normal University, Shanghai; [2]Aerospace Information Research Institute, Chinese Academy of Sciences, Beijing; [3]College of Finance and Economics, Nanchang Institute of Technology, Nanchang, Jiangxi, China

Abstract

Terrestrial laser scanning (TLS) is a promising technology for quantity checking huge grain stocks with low cost, light workload and high efficiency. Existing applications of TLS in bulk grain measurement and quantification lack the ability to capture complete structural information of grain bulks and thus will result in large errors. In this paper, we propose a bi-temporal TLS scheme for fast 3D modeling and accurate volume measurement of bulk grains stored in large warehouses. The scheme uses bi-temporal multi-site TLS datasets acquired under both empty and full or high loading conditions to obtain complete surface information about grain bulk's structure. In order for a grain bulk's all external surfaces and the 3D volumetric model reconstructed therefrom to be automatically derived from the bi-temporal TLS dataset, several dedicated methods are developed for the scheme. A fully automated marker-free strategy exploring structurally semantic information inherent in the large grain storehouses is adopted to register multi-scan TLS point cloud data captured in large-scale granary scenes. Also, a local minima-based region growing technique is devised to extract underlying surfaces from a granary scene point cloud model. Experiments show that the proposed 3D modeling and volume measurement scheme can work effectively and quickly in TLS-based granary field applications and repeated test data demonstrate its correctness, repeatability and accuracy. Compared with the conventional manual measurement approach, the bi-temporal TLS scheme can not only achieve much higher measurement precision, but also greatly improve efficiency by significantly reducing cost, workload, and manpower. It has good potential for use in the area of nationwide grain inventory inspection in China.

Correspondence: Yinghong Tian, School of Communication and Electronic Engineering, East China Normal University, Shanghai, China. E-mail: yhtian@ee.ecnu.edu.cn.

Key words: bulk grain measurement; grain storehouse; point cloud; markerless registration; surface extraction.

Contributions: XH, methodology, data analysis and original draft writing; TX, data curation and original draft writing; LY, FW, experimental design and data acquisition; YF, manuscript review and editing; YT, research coordination and manuscript review. XH and TX contributed equally.

Conflict of interest: the authors declare no potential conflict of interest.

Funding: none.

Acknowledgments: this work was supported in part by the National Natural Science Foundation (NSF) of China (Grant No. 41771475) and in part by the Special Scientific Research Fund of Public Welfare Profession of China (Grant No. 201313009). All the authors approved the final version to be published.

Received: 22 March 2023.
Accepted: 19 April 2023.

Journal of Agricultural Engineering 2024; LV:1555
doi:10.4081/jae.2024.1555

Introduction

As one of the most significant tasks for grain reserve management, the national grain inventory inspection in China plays a vital role in structure adjustment of agricultural production, macroscopic regulation of grain markets and guaranteeing of national food security. In grain inventory inspection, the quantity (or weight) of grains needs to be measured accurately and quickly, and yet it is a difficult technical task. Conventionally, an approach known as the "volume-density method" is applied in the nationwide grain inventory practice of China (Ren, 2007), which performs the calculation of the grain weight by multiplying the grain bulk's volume by its average density. Thus, how to measure the volume of stored bulk grains is one of the two critical issues in estimating the grain quantity using this method. In the conventional way, the grain bulk is assumed to be a three-dimensional (3D) object with some regular geometrical shape (*e.g.*, a rectangular cuboid, a cylinder or a circular cone), and then basic dimensions of the grain bulk, measured with steel or leather tapes, goniometers and other tools, could yield the value of the bulk's volume according to routine volume computation formulas for standard geometrical shapes (Ren, 2007). Yet for the irregular grain bulks (before leveling or during charge and discharge process), application of this method necessitates manual forming and geometric approximation, which implies low efficiency and high cost by manpower and will lead to considerable errors. In summary, this conventional method is a fast estimation technique for grain quantity with low cost, light workload and high efficiency, but it cannot achieve high precision and is only suitable for quantity checking of grain bulks with regular shapes.

Terrestrial laser scanning (TLS) is a relatively low-cost optical

surveying technique in 3D spatial data acquisition, which allows measured objects to be digitally captured with unprecedented resolution and accuracy (Buckley *et al.*, 2008; Reshetyuk, 2009; Chen *et al.*, 2018). The spatial resolution of terrestrial laser scanners is high with a density to be several thousand or even more points per m^2, and their accuracy is sufficient to obtain very detailed information about the objects' structure (Lumme *et al.*, 2008). Also, tripod-mounted TLS systems are considered to be practical for operational use (O'Neal, 2014). The instrument's portability, ease of use, low expenses and sufficient accuracy open the possibility of application of the laser scanning technology in the field of close-range sensing and measurement.

In recent years, TLS has been commonly used in different engineering survey applications, including terrain and landscape mapping (Huising and Pereira, 1998), historical and cultural heritage documentation (Montuori *et al.*, 2014), and civil building modeling (Pu and Vosselman, 2009), *etc*. Among significant experiences based on the use of TLS, Barreca *et al*. (2017) adopted advanced 3D surveying techniques (*i.e.*, TLS) on agri-food facilities to create a three-dimensional parametric model for the purpose of energy performance assessment in agri-food buildings; TLS was also used to calculate the volumes of outdoor manure piles (OMPs) in a Korean OMP investigation project (Park *et al.*, 2021). Theoretically, TLS can also be applied in volume measurement of bulk grains stored in large warehouses, but the literature relating to this area is rare and only a few scattered academic papers or technical reports can be found. For example, Liang and Sun (2011) focused their presentation on a flow of methods to fast and accurately obtain the grain storage's internal structure and further estimate the grain volume, covering preprocessing, segmentation, feature identification, registration, surface reconstruction and volume estimation. Similarly, a laser scanning system dedicated to the measurement of grain volume in the large storage tank, which consists of a laser scanner, a stepping motor, a power supply and frame assembled with slotted angle iron, was described in detail by Zeng *et al*. (2012). Zhu *et al*. (2012) reported their experiments for measuring the volume of irregular grain bulks using laser scanning technology. An online measuring system for stored bulk grain using a 3D laser scanning technology was proposed by Shao *et al*. (2016). These systems can reconstruct the grain's surface by conducting contactless measurements of 3D coordinates of surface points in a granary and estimate the volume of the stored grain bulk based on a derived surface model. Due to the inability of such systems to capture hidden surfaces underlying the stored bulk grain, volume estimation based solely on upper surface models would result in large errors.

Accurate volume measurement of bulk grains should utilize 3D volumetric models constructed from data from multiple laser scans acquired at different times and different sites. Considering the difficulty of obtaining complete information on the granary structure or grain surfaces by single-site scanning (or one viewpoint) and other factors (*e.g.*, occlusion effect, uneven density and discontinuous spatial distribution characters, *etc*.), multi-site scanning (or multiple viewpoints) is required (Liang and Sun, 2011). Besides the scans taken under high or full loading conditions to capture grain surfaces, it is necessary to perform laser scanning in an empty storehouse with no grain loaded to acquire the internal structure of the granary. As the underlying surfaces can be derived from the granary's structural information, a volumetric model depicting the grain bulk's 3D shape could be reconstructed by merging these scanning data collected under different loading conditions.

In this paper, we propose a TLS-based 3D modeling and volume measurement scheme for bulk grains stored in large warehouses. This scheme utilizes bi-temporal multi-site TLS datasets acquired under both empty and full or high-loading conditions to obtain complete surface information about grain bulks. In order for a grain bulk's all external surfaces and the 3D volumetric model reconstructed therefrom to be automatically derived from the bi-temporal TLS dataset, several dedicated methods are developed for the scheme. A fully automated marker-free strategy exploring structurally semantic information inherent in the large grain storehouses is adopted to register multi-scan TLS point cloud data captured in large-scale granary scenes. Also, a local minima-based region growing technique is devised to extract underlying surfaces from a granary scene point cloud model. The proposed scheme is experimentally applied to bi-temporal TLS data acquired in large storehouses of several different grain reserves across China and its correctness and accuracy is evaluated by repeated TLS measurement tests.

Materials and Methods

Study area and data acquisition

The study was conducted in the Dadushe Grain Reserve Depot located in Tongzhou District, Beijing, China (Figure 1a). This

Figure 1. Experimental granary and terrestrial laser scanning data acquisition. (**a**) A snapshot of Dadushe Grain Reserve depot where experiments took place; (**b**) front view of the large grain storehouse; (**c**) scanning experiment under an empty condition; (**d**) scanning experiment under a full condition.

depot contains more than 10 large granaries. Figure 1b shows an example granary, which is a large rectangular storehouse, about 50 meters long and 26 meters wide. The total height of the grain storehouse is about 10 meters and its grain pile height is 6 meters. Terrestrial laser scans were performed in each grain storehouse to generate 3D point cloud data which reflects the grain bulk's geometry and the storehouse's internal structure.

In order to collect bi-temporal data, laser scanning experiments were carried out in two different temporal phases where a large grain storehouse shows great differences in terms of loading conditions: one set of laser scans was performed in an empty condition with no grain loaded to capture hidden surfaces underlying the grain bulk (Figure 1c) while the other set of scans were taken under high loading conditions to capture grain surfaces (Figure 1d). Also, multi-site scanning is needed to fully cover a large-scale scene. Prior to scanning experiments, measure stations (*i.e.*, the sites where individual scans are performed) were reasonably arranged according to the granary structure, the shape of the object and the effective range of the instrument. Two sets of four-site raw laser scanning data acquired under different loading conditions are shown as an example of bi-temporal TLS data in Figure 2a-b, respectively. In this example, the layout of measuring sites for the 3D laser scanner is illustrated in Figure 2c. Scanning measurements were performed at four sites roughly along the centerline of the grain storehouse successively in both experiments.

The terrestrial laser scanner used for the experiments is an application-specific 3D laser scanner designed for grain inventory inspection ASQ-MStar8000i, as shown in Figure 1c-d. It is a class 1 eye-safe laser product operating with a wavelength of 1550 nm, an emergent spot diameter of 3.25 mm and a beam divergence of no more than 0.4 mrad, which generates a point cloud of up to 13,000 points per second with a range of up to 80 m and a typical accuracy of ±5 mm. The point cloud is a data set comprised of three-dimensional coordinates (in millimeters) of all laser footprints hitting the grain or other objects' surfaces. The derived point cloud data in this study assumed the *x*-*y*-*z* Cartesian coordinate system and permitted an average footprint density of 195 pt/m^2. A fixed scanning rate of 8,000 points per second was used for all experiments. As the maximum number of points contained in the data generated by every measure station is 1.5 million in this study, the surveying time for a single scanning experiment would not exceed 5 minutes. Considering the length of the grain storehouse is less than 60 meters, the 3D laser scanner was also set to cut points outside the optimal range (0.2~60 m) to ensure millimeter-level measurement accuracy.

Methodological workflow

We propose a TLS-based schematic flow of 3D modeling and volume measurement methods for bulk grains stored in large warehouses. In the entire scheme, a bi-temporal multi-site TLS dataset will go through a series of mathematical processing tasks, such as data preprocessing, registration, surface extraction, 3D reconstruction and volume calculation. The methodological workflow is illustrated in Figure 3, where the ellipses represent data or models and the rectangles represent processes or calculations. Each essential processing stage will be described in detail in the following part of this section.

Data preprocessing

Due to various environmental disturbances (*e.g.*, the interference from outside light), instrumental vibrations and operational factors in the data acquisition process, noisy points will inevitably be introduced into the generated point cloud datasets. In addition to these noisy data produced by random factors, the concave geometry's occlusion effect or variability in the measurement might lead to sparse outliers (namely the data points further away from the sample mean than what are deemed reasonable) which corrupt the reconstructed point cloud model even more. The noisy point cloud complicates the estimation of local point cloud characteristics such as surface normals or curvature changes, leading to erroneous values, which in turn might cause subsequent point cloud processing tasks (*e.g.*, registration, segmentation, feature extraction and surface reconstruction, *etc*.) failures. Moreover, the amount of data captured directly by the 3D laser scanner is usually very large and, to a certain extent, redundant, which seriously affects the speed and accuracy of the subsequent processing. Therefore, it is necessary to preprocess the raw point cloud data in a proper way.

In the preprocessing phase, filtering algorithms are utilized to remove outliers and down-sample the point cloud. We adopt the statistical outlier removal method to remove the noise and outliers

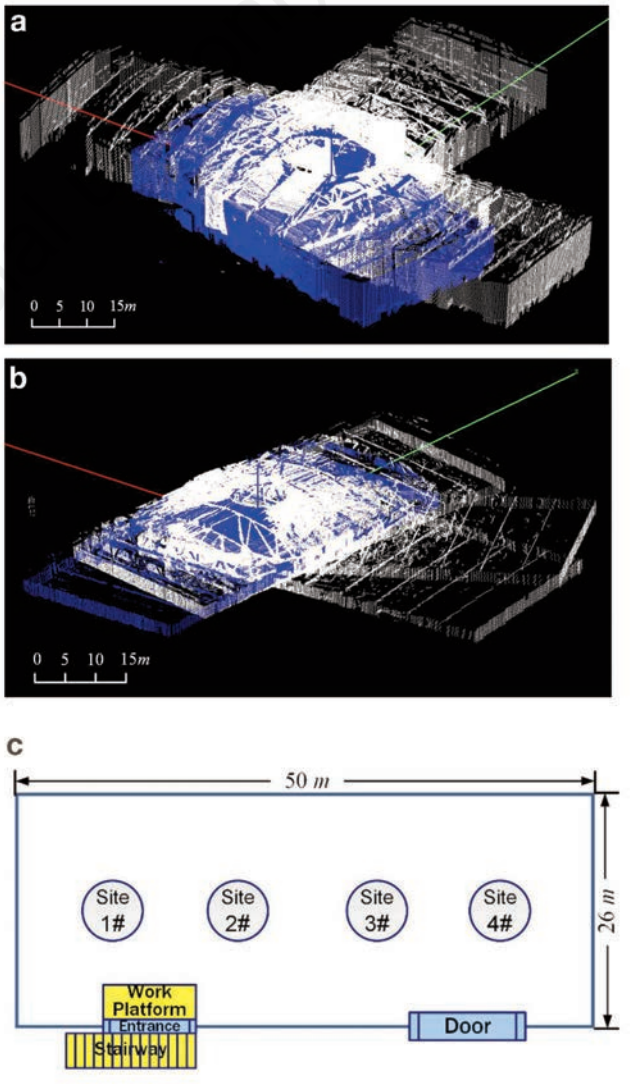

Figure 2. An example of acquired bi-temporal multi-site 3D terrestrial laser scanning data for an experimental grain storehouse. (**a**) Four-site raw point clouds under an empty condition; (**b**) four-site raw point clouds under a full condition; (**c**) site distribution.

(Rusu, 2009). The basic idea behind this method is to perform a statistical analysis on each point's neighborhood in the dataset and trim those that do not meet a certain criterion. For each point, its average distance to the *K* nearest neighbors is computed. By assuming that, the resulting distribution is Gaussian with a mean and a standard deviation, all points whose average distances are outside an interval defined by the global mean and standard deviation can be considered as outliers and trimmed from the dataset. The voxel grid method is also used for point cloud down-sampling to reduce the number of points while keeping the contour of the point cloud unchanged, aiming to improve the running speed of subsequent key algorithms, such as feature recognition and point cloud registration (Rusu, 2009). This technique creates a 3D voxel grid (*i.e.*, tiny 3D boxes in space) over the point cloud data and then in each voxel, all the points present will be approximated with their centroid. Figure 4 illustrates the effects of the statistical outlier removal and the voxel grid-based down-sampling: the original point cloud is shown in Figure 4a, while the resultant dataset after statistical analysis and filtering and the down-sampled dataset with the compression ratio of approximately 1/4 are in Figure 4b-c, respectively.

Multi-site registration

Multiple laser scans acquired at different sites are needed to fully cover large-scale granary scenes in full detail. Because each scan refers to its own local coordinate reference, a prerequisite for any further processing of such data is the registration process which aligns all individual scans into a uniform coordinate reference system to obtain one large point cloud of the complete scene. To circumvent an artificial marker-based strategy that is significantly time-consuming as marker positioning is rather troublesome and requires careful planning, the automatic marker-free registration method for multi-scan granary scene point cloud data presented in (Hu *et al.*, 2021) is adopted in this study. The framework of the markerless method follows the common procedure to split the entire registration into global alignment (*i.e.*, coarse registration) and fine registration. To tackle the correspondence problem, which is at the core of a registration task, the geometrically semantic information inherent in grain storehouses is explored in the stage of global coarse alignment. A point-to-plane iterative closest point algorithm presented by Chen and Medioni (1992) is used in the fine registration step to minimize the cumulative distance between point clouds of different scans.

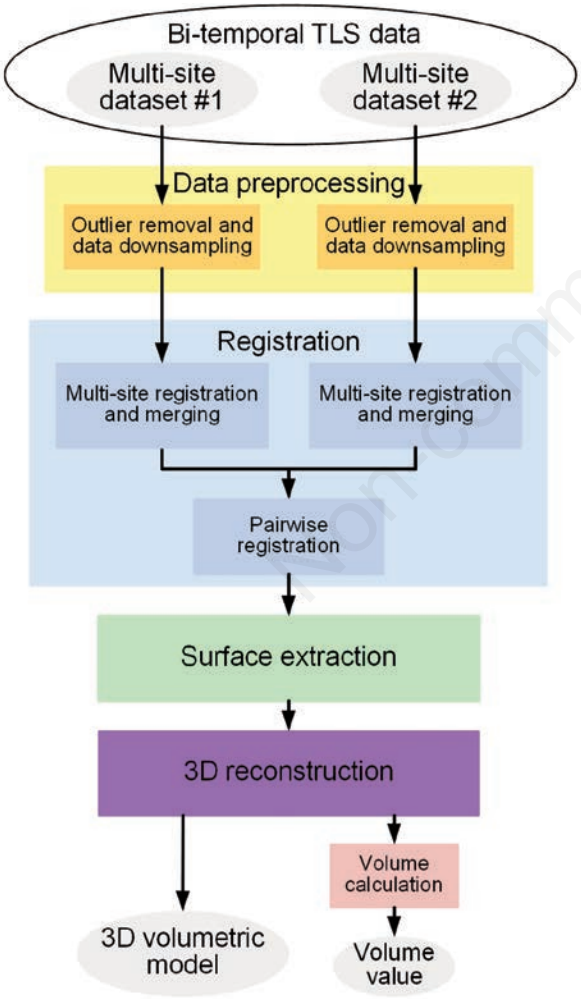

Figure 3. Workflow of the proposed bi-temporal terrestrial laser scanning scheme for 3D modeling and volume measurement of stored bulk grains. TLS, terrestrial laser scanning.

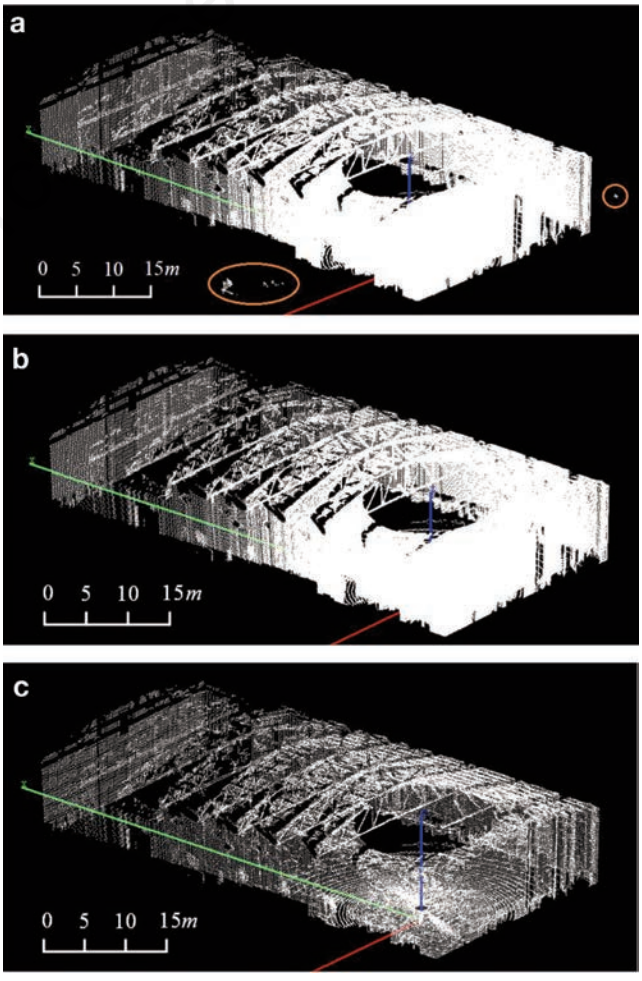

Figure 4. An example of point cloud filtering (outlier removal) and data down-sampling. (**a**) Original point cloud data; (**b**) the filtered point cloud after statistical analysis; (**c**) down-sampled point cloud using the voxel grid method (Leaf size=0.1 m).

Prior to the coarse alignment is the step of extraction of geometrical features. There are 3 types of features of interest in a typical grain storehouse: point features (*e.g.*, vertices and corner points), line features (*e.g.*, edges and intersection lines of surfaces) and surface features (*e.g.*, walls, ground and grain surfaces), as illustrated in Figure 5. In these geometrical features, the corner lines refer to the joint lines of adjacent walls and the corner points, *i.e.*, intersections of the vertical corner lines with the roof, are used as semantic features to establish point-to-point correspondences between different point clouds in coarse registration. Extraction of corner points begins with determining the approximate horizontal positions of four corner lines by measuring the rectangularity of a quadrilateral region formed by the projected 2D point set of a specific scan. Then each corner point is located by searching for the point with the highest elevation in the vicinity of each corner line.

The global coarse alignment is a crucial step of the whole registration process, which roughly aligns point clouds with a precision that avoids the following fine registration from getting stuck in a local minimum. In this step, the extracted semantic features (*i.e.*, corner points) are mathematically modeled as a 4-element ordered set:

$$G^{(i)} = \{G_i, G_{(i+1)\%4}, G_{(i+2)\%4}, G_{(i+3)\%4}\}, \quad (1)$$

where the symbol % represents a modulus calculation and $i \in \{0,1,2,3\}$, indicating the ordered set starts with the point with the index of i. In order to establish reliable correspondences between the geometrical features from two different scans with a sufficient overlap of point clouds, a simple enumeration process is employed to match feature points by anchoring the target scan's feature set G_q and iteratively reordering the source scan's feature set G_p, where the matching pair with the maximum LCP (largest common point-set) measure (Yon *et al.*, 2017) is regarded as the solution for the global coarse alignment between two scans. The idea behind the enumeration process is to perform alignment tests for all possible matching pairs of two sets of geometrical features extracted from the source scan P and target scan Q, respectively. Each aligning transformation is assigned a score based on the number of common points that are brought into alignment up to a threshold. Over all trials, the matching pair with the optimum transformation (*i.e.*, the transformation with the best score) is regarded as the solution for the global alignment between two different point clouds. Figure 6a-b shows the multi-site registration results of the above-mentioned method for TLS point cloud datasets acquired under empty and full conditions respectively, in which different colors indicate points from different scans. For a detailed description of the automatic marker-free registration method, please refer to Hu *et al.* (2021).

Extraction of ground and grain surfaces

The 3D volumetric modeling of bulk grains stored in large warehouses necessitates the extraction or segmentation of ground surfaces and grain surfaces from the point clouds of different laser scans taken under empty and full loading conditions respectively. Segmentation in point cloud data is difficult because the points are usually unorganized, incomplete, noisy, sparse, have inconsistent point density, and in addition, the surface shape can be arbitrary with sharp features. Segmentation methods can be divided into two categories: border-based approaches and region-based approaches (Nurunnabi *et al.*, 2012). In a border-based approach, boundary and edge points are first identified and then the extracted border points are used to segment the surface according to different saliency features (*e.g.*, curvatures, normal vectors or local neighborhood distribution) (Wang *et al.*, 2018). Region-based approaches use local neighborhood properties to seek the homogeneity within a specific feature or find variation among the features, and

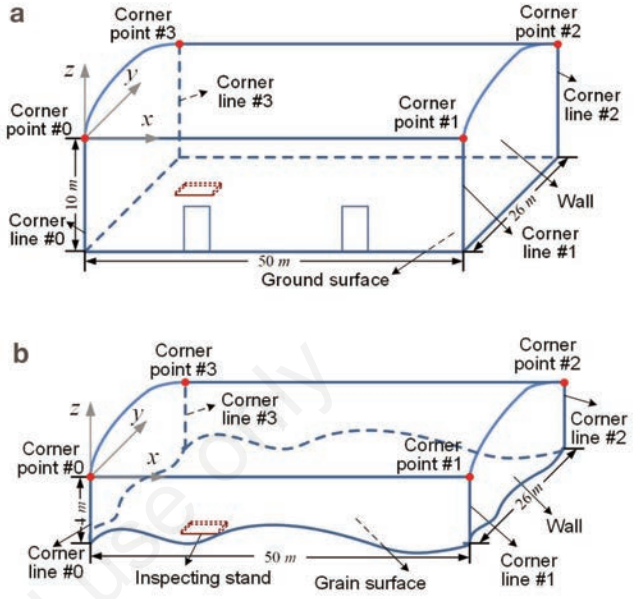

Figure 5. The geometric model of the large grain storehouse. (**a**) An empty condition; (**b**) a full condition.

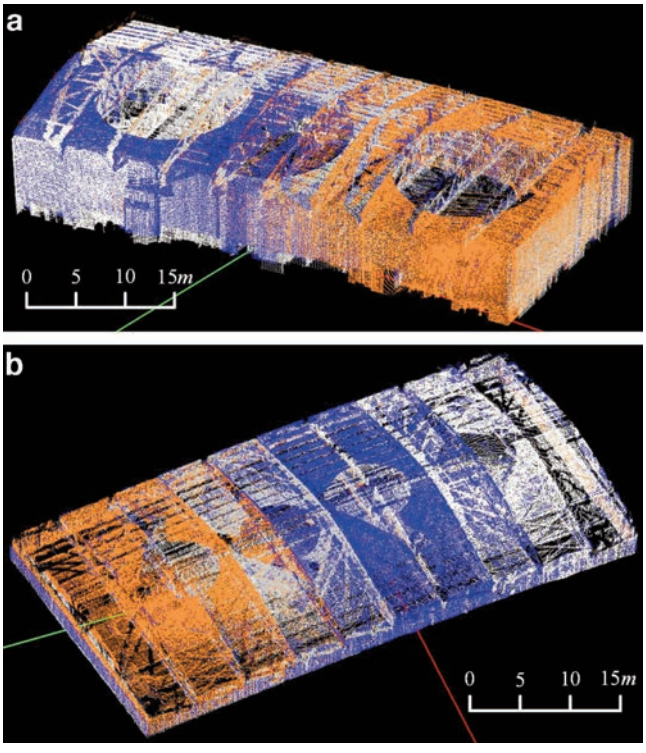

Figure 6. Multi-site registration results for 4 terrestrial laser scanning point clouds with different colors (black, yellow, grey and blue) representing points from different scans. (**a**) An empty condition; (**b**) a full condition.

merge the spatially close points. Region growing, as a kind of simple region-based method, is widely adopted for the extraction of feature surfaces in 3D point cloud data (Hu *et al*., 2017). Region-based segmentation can also resort to clustering algorithms or the random sample consensus algorithm (Wang *et al.,* 2018). In general, region-based methods are more robust to noise than border-based ones due to the use of global information.

Actually, the acquired TLS data has one property that should not be ignored in working out a surface segmentation scheme for the point cloud in the application of bulk grain measurement. The z-axis of its acquisition coordinate system is vertical (*i.e.*, along the direction of gravity) due to the automatic leveling ability inherent in the laser scanner, and thus the ground or grain surface in the point cloud model can be regarded as an underlying surface, any point on which has the lowest elevation in the vicinity of the vertical line through it. In this work, we propose a local minima-based region-growing technique to segment the underlying surface from a granary scene point cloud model. The conventional region-based methods cannot dispense with the time-consuming pointwise computation and a more crucial issue in directly applying the region-based segmentation is how to determine the initial seed points, whose numbers and locations would strongly influence subsequent processing steps. A "divide and conquer" strategy is adopted in this technique to improve computational efficiency by partitioning the 3D space containing the point cloud model into small vertical units and perform a standard region-growing process in each partition. The initial seed point for each region's growing process can be determined by finding the local minimum point in terms of elevation in a specific vertical unit. The first step is to perform a 3D space division of the TLS point cloud captured in a granary scene. Create an axis-aligned minimum bounding box for the 3D dataset and divide the box into many vertical cuboids of the same size. Let c_x, c_y and c_z denote the cuboid's sizes in the *x*-, *y*- and *z*-axes, respectively, and they are determined as

$$c_x = B_X/N_{div}, \quad (2)$$

$$c_y = B_Y/N_{div}, \quad (3)$$

and

$$c_z = B_Z, \quad (4)$$

where B_X, B_Y and B_Z are the edge lengths of the 3D bounding box in the directions of *x*-, *y*- and *z*-axes, respectively, and N_{div} is named the space division coefficient, which assumes a positive integer, for example, 8, 16, 32, *etc*. The basic idea of the 3D space division of the point cloud model is illustrated in Figure 7a-b.

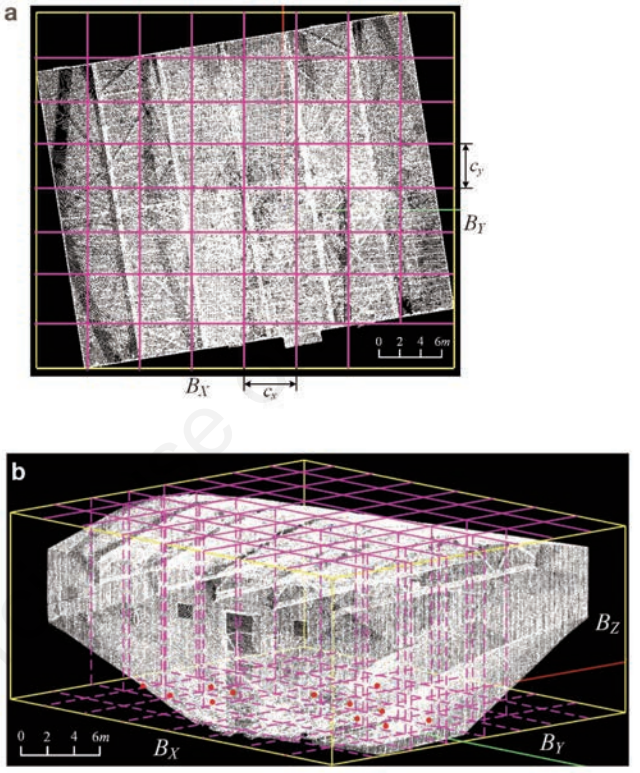

Figure 7. An example of the 3D space partition of the granary scene terrestrial laser scanning point cloud (N_{div}=8). (**a**) Top view; (**b**) divide the 3D axis-aligned bounding box containing the point cloud model into vertical cuboids with identical sizes. The local minimum points are marked in red.

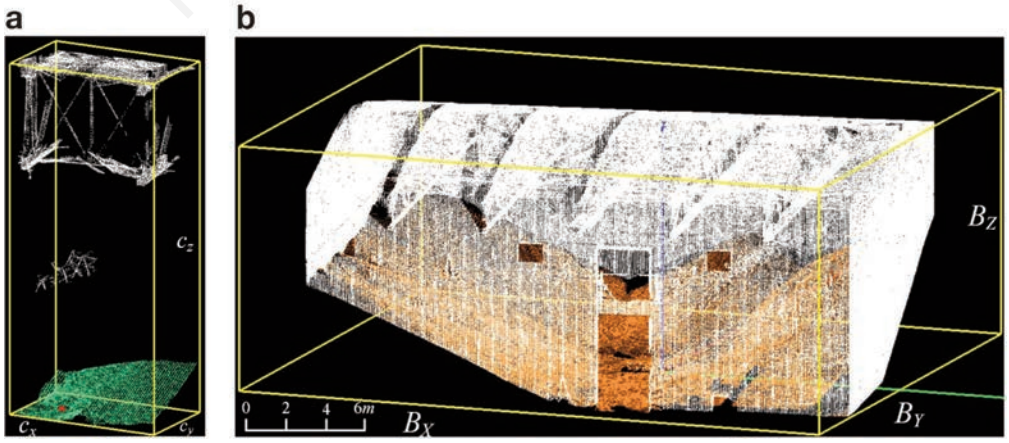

Figure 8. Extraction of the granary surface in a granary scene point cloud model. (**a**) Extracting the underlying surface (rendered in green) in a vertical cuboid by exploiting a region-growing process. The red dot represents the local minimum point of the cuboid; (**b**) concatenating neighboring regions to form a complete grain surface (rendered in orange).

For each vertical cuboid, locate its local minimum point that is defined as the point with the lowest elevation inside it, as shown in Figure 7b. In order to eliminate the deleterious effects of noise, the local minimum point can be determined by finding M_{lm} (it is a predefined parameter) lowest points in a specific cuboid and then taking the average of these points' coordinate values.

Next, a region-growing method is employed in each vertical cuboid to extract its underlying surface. In this step, a surface region begins its growth from the local minimum point in the specific cuboid and the points that are close enough in terms of the distance and smoothness constraints are clustered. The region-growing method based on the distance and smoothness constraints is described as follows:

i) construct a subset S from the point set contained in the vertical cuboid: delete points whose heights are greater than $z_{min} + (c_z - z_{min})/2$ (z_{min} is the coordinate value in the z-dimension of the local minimum point) and sort the remaining points by their height values. Set the local minimum point as the initial seed and add it to the current seed list L_S, and then start the process of region growing;
ii) for every seed point in L_S, find K nearest neighbors in S. Each neighbor is tested for the angle between its normal and the normal of the current seed point. If the calculated angle θ is less than a predefined threshold value θ_{th} (set to 45°), the neighboring point is added to the current seed list L_S and the current region R_c, and then removed it from S. Current seed is also removed from L_S;
iii) repeat Step 2 until the current seed set L_S becomes empty, which means the algorithm has grown a complete region that is considered to be the underlying surface in the vertical cuboid. The algorithm is terminated when all the points contained in the underlying surface are extracted from the point set S.

Finally, the grown regions in all vertical cuboids of the 3D bounding box are merged to form the underlying surface of a granary scene point cloud model. Figure 8 presents an example of extracting the granary surface from a TLS point cloud captured in a grain storehouse by merging all regions grown in each vertical cuboid. The underlying surface in a specific vertical cuboid is extracted by applying a distance and smoothness constraints-based region growing method, as illustrated in Figure 8a. Figure 8b shows the result of the final merging operation.

3D modeling of grain bulks

The 3D volumetric modeling of a grain bulk is essentially to reconstruct the external surfaces of this grain bulk. The grain bulk stored in a large warehouse mainly consists of a grain surface, a ground surface and/or several wall surfaces. As the surfaces cannot be reconstructed altogether in a single scanning experiment, deriving a volumetric model of the grain bulk from these surfaces implies the simultaneous use of bi-temporal TLS datasets, which are acquired under empty and full conditions, respectively. For either dataset, multi-view registration is needed for all scans in it and generates a complete point cloud model by merging all the registered scan data. Then a pairwise registration is performed on the two partially overlapping point cloud model merged from both registered datasets, as illustrated in Figure 9a. So, the underlying surfaces of the bi-temporal granary scene point cloud models can be extracted in a uniform coordinate system. Points above the grain surface in both models are removed and the remaining points constitute a point set that precisely characterizes the grain bulk's external surfaces. Figure 9b shows a point set for the grain bulk derived in the way described above. Finally, a greedy projection triangulation (Marton *et al.*, 2009) is adopted to perform 3D surface reconstruction on the derived point set. The ultimate 3D volumetric model for the grain bulk is shown in Figure 9c.

Volume calculation

In the process of 3D volumetric modeling, the triangulation operation yields a surface mesh model for the grain bulk by decomposing each bounding surface that envelops the 3D point set into numerous facets. Triangular facets in the grain and ground surfaces are utilized to estimate the volume of the point cloud model representing a grain bulk's 3D shape. In order to speed up the computation, we devise a simple algorithm to calculate the grain bulk's volume based on facet projection, which is illustrated in Figure 10. Firstly, a reference plane parallel to the *xoy* plane is inserted into the mesh model. Each triangular facet in the grain and ground surfaces is projected onto the reference plane and an approximate triangular prism is then created with this triangle and its projected copy. Thus, the 3D mesh model can be divided into numerous seamless approximate tri-prisms and its volume can be computed by summing up the volumes of all triangular prisms:

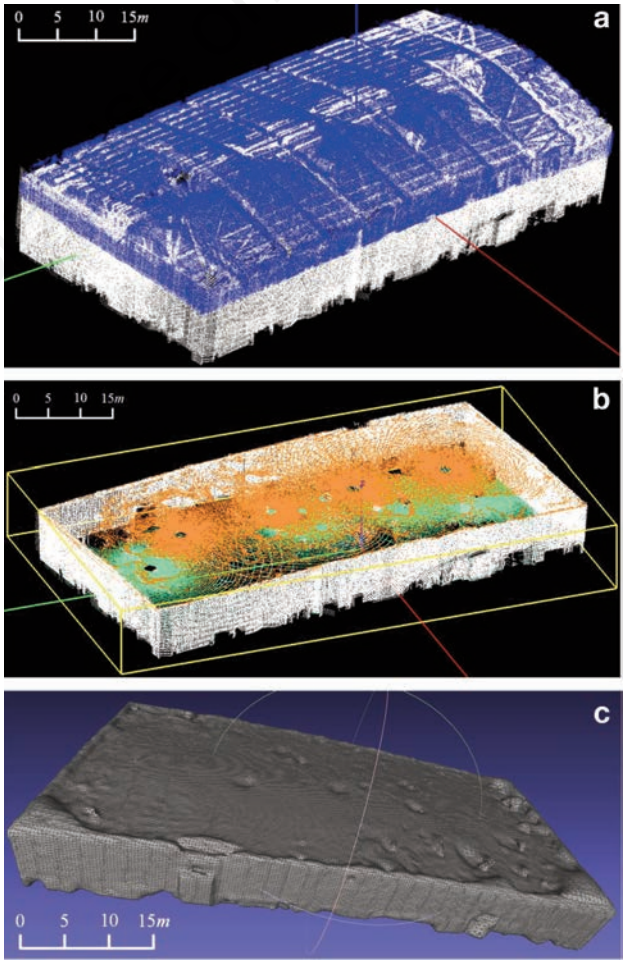

Figure 9. An example of generating 3D volumetric model for a grain bulk. (**a**) Pairwise registration for bi-temporal granary scene point cloud models. Different colors represent different terrestrial laser scanning datasets acquired under empty and full conditions, respectively; (**b**) the point set depicting the grain bulk derived from bi-temporal point clouds. Points in the grain, ground and wall surfaces are rendered in orange, green and white, respectively; (**c**) the 3D model is reconstructed by a greedy projection triangulation method.

$$V = \sum_{i=1}^{N_{tf}} p_t(i)S_t(i)h_t(i) + \sum_{j=1}^{N_{bf}} p_b(j)S_b(j)h_b(j), \quad (5)$$

where, N_{*f} is the number of triangular facets, $p_*(i)$ is called the polarity index, $S_*(i)$ denotes the area of triangle projected onto the reference plane by the facet contained in the grain or ground surface, $h_*(i)$ denotes the height of each tri-prism, and the subscript t or b means that the mathematical quantity is related to the grain or ground surface, respectively. The polarity index $p_*(i)$ takes only the values of ±1. For a triangular facet in the grain surface, if its centroid is above the reference plane, $p_t(i)$ takes the value of +1, otherwise it takes the value of -1. For any facet located in the ground surface, the reverse applies.

Software design

The overall mathematical processing contained in the scheme is performed on a C/C++ software system for TLS data processing that we specifically developed for a research project for Chinese grain industry. The software system was designed with *Qt*, which is a cross-platform GUI framework for desktop, embedded and mobile application development. For the sake of convenient development and maintenance, the object-oriented modular structure design was adopted by the software system, where various functional modules were integrated by means of static link libraries (*lib*) or dynamic link libraries (*dll*). Graphics rendering application programming interfaces in OpenGL were utilized for visualization of 3D point clouds and drawing other 3D shapes (*e.g.*, mesh models and other 3D shapes) on screen. As for the implementation of 3D processing algorithms, the software integrated some modular libraries provided by the Point Cloud Library (PCL), which is an open-source library of algorithms for point cloud processing tasks and 3D geometry processing, such as occur in three-dimensional computer vision (Rusu and Cousins, 2011). Generic techniques for data representation, nearest neighbor search, feature description, point classification, filtering, segmentation, interpretation, modeling and so on, were implemented with the methods and classes contained in PCL's modules, while the application-specific algorithms, such as geometrical feature extraction, pairwise registration, surface isolation and volume calculation, were implemented from scratch.

The software makes it easy to create 3D polygon models and meshes from scanned point cloud data depicting a large-scale granary scene. It mainly consists of six modules: Ganary3D, OGL, G3dBasic, G3dPlugin, IO and Algorithm. Key features of this software include: rendering and manipulation of 3D data, surface analysis, distance measurement and volume calculation, automatic alignment of scanned point clouds, automatic conversion of point cloud data to polygons, automatic surface segmentation, output matching with standard file formats, *etc*. Source codes of the software's non-commercial version can be available free of charge on request.

Results

Parameter setting

As described in the previous section, the proposed flow of methods has several parameters that must be specified before a scanning experiment. These parameters can control the qualities of filtering, registration, segmentation and surface reconstruction and will have a significant influence on the overall performance in terms of accuracy and speed. Specifying the control parameters before data processing is also an important task of the experiments. The global parameter settings depend mainly on the size of the storehouse, the complexity of the scene, the point-cloud density, and the computational cost. Scheme-specific parameters used in the experiments are listed in Table 1.

The voxel grid filter's leaf size S_{leaf} determines the sampling rate or compression ratio when the original TLS data is down-sampled. A high sampling rate can speed up the processing process, but will lead to loss of accuracy. Setting S_{leaf} to $0.1m$, which implies a sampling rate of approximately 1/4 can be achieved, is a tradeoff between time and performance. For the sake of reliable registration, the slicer number N_{slic} should take a large number (*e.g.*, 1024) to ensure sufficient point samples for straight-line fitting-based edge outlining. The same principle also applies to the setting of the other two parameters used in the registration process: search radius R_S and uncertainty measure δ. The space division coefficient N_{div} controls the quality and time cost of underlying surface segmentation. A large value of this parameter could achieve high computational efficiency for this task but would degrade its robustness to noises. Thus, we take a small integer 16 for N_{div} to limit the completion of surface segmentation to less than 1 minute while achieving enough good results.

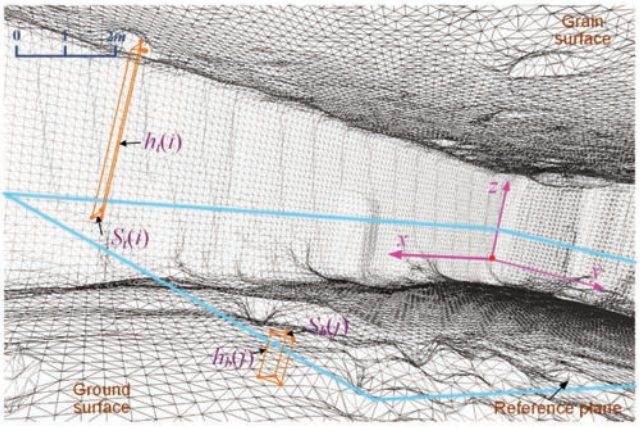

Figure 10. Triangular facet projection-based volume calculation for a 3D surface mesh model of bulk grains stored in a large warehouse.

Table 1. Parameter setting for terrestrial laser scanning experiments.

Parameter	Description	Value
S_{leaf}	Leaf size for the voxel grid filters used in data preprocessing	0.1 m
N_{slic}	Number of point slicers for edge outline sampling used in registration	1024
RS	Search radius for determining geometrical feature points used in registration	0.5 m
δ	Uncertainty measure for point pattern matching between two-point sets used in registration	10 cm
N_{div}	Space division coefficient used in segmentation	16

Experimental results

A total of 8 sets of bi-temporal TLS data were selected from the experiments to demonstrate 3D modeling and volume measurement results. We feed these sets of data into the dedicated software system, which implies that a series of mathematical processing procedures described in Section 2 will be performed on them. Figure 11 shows the 3D volumetric models of grain bulks reconstructed from 8 sets of bi-temporal TLS point cloud data collected in different rectangular storehouses. The first two models are for regular grain bulks, while the other six models are derived from grain bulks with irregular surfaces or even irregular geometrical shapes. Utilizing these 3D models, we can calculate the volumes of grain bulks, as shown in Table 2. In contrast, the volume values of these grain bulks acquired by the conventional manual measurement method are also listed in Table 2. Comparison results show the relative errors of calculated volumes in two different ways were no more than 4%.

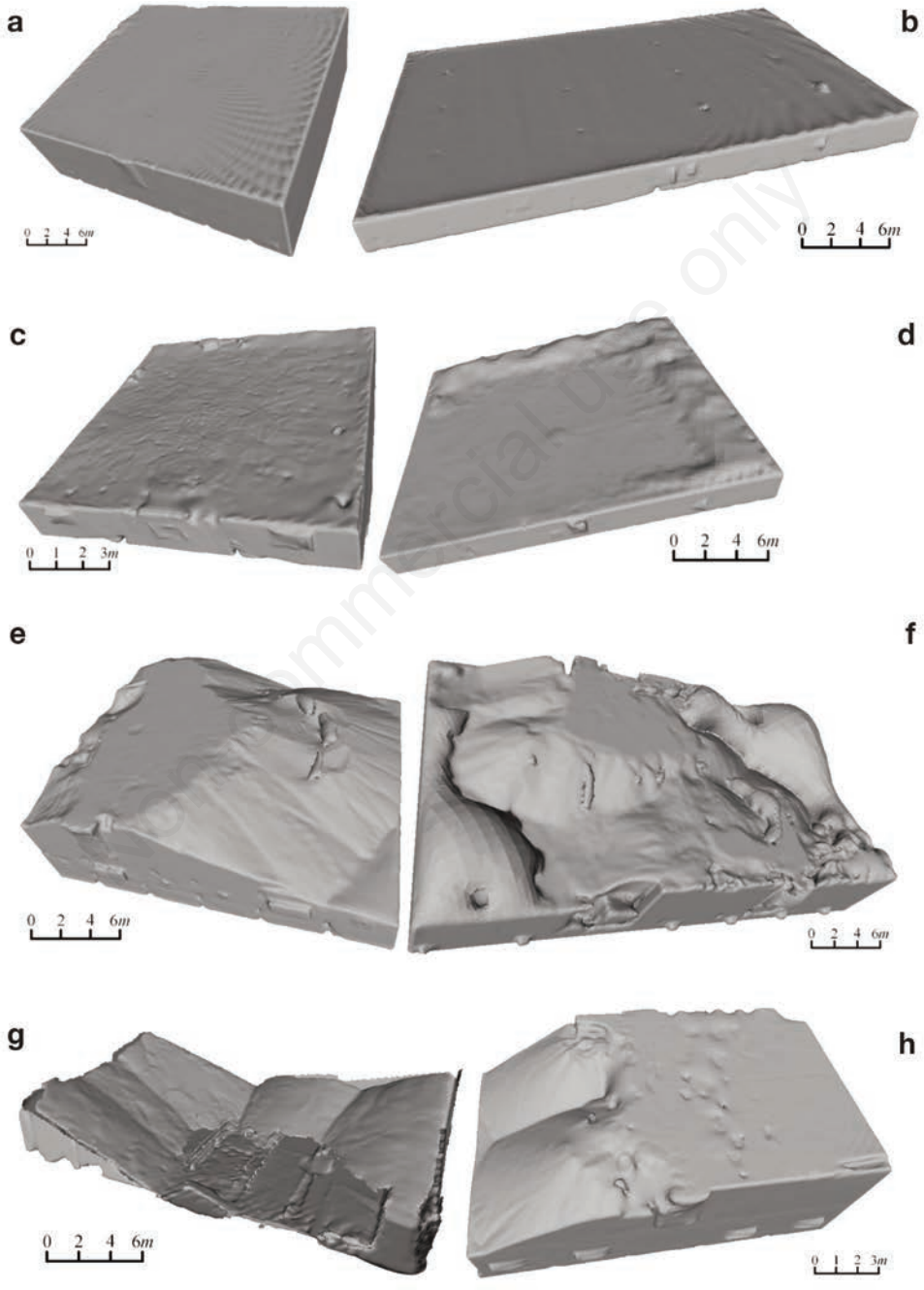

Figure 11. Reconstructed 3D volumetric models from bi-temporal terrestrial laser scanning point cloud datasets captured in 8 different grain storehouses. (**a**) The model for Dataset #1; (**b**) the model for Dataset #2; (**c**) the model for Dataset #3; (**d**) the model for Dataset #4; (**e**) the model for Dataset #5; (**f**) the model for Dataset #6; (**g**) the model for Dataset #7; (**h**) the model for Dataset #8.

Time estimation

To demonstrate the time performance of the proposed bi-temporal TLS scheme, its time costs should be evaluated. The total time to complete the whole workflow described in Figure 3 comprises two parts: data acquisition time and data processing time. The data acquisition time includes all surveying time at different scanning sites under two different loading conditions. The data processing time refers to the CPU running time for each step of the proposed mathematical processing flow. We have run the TLS data processing software on an HP® workstation computer with a 2.5 GHz Intel® Core™ i7-6700 processor, 16 GB of RAM and 2 TB of solid-state drive. Table 3 lists the details of time costs for each task of the proposed TLS scheme performed on 3 sets of bi-temporal point cloud data collected in different rectangular storehouses. From Table 3, we can see that it takes only tens of minutes to use the bi-temporal TLS scheme for 3D modeling and volume measurement of stored bulk grains, which is much faster than the conventional manual measurement method.

Discussion

Correctness verification

Although Table 2 indicates the results produced by the TLS-based measurement are consistent with those by the manual measurement, it is insufficient to verify the correctness of the proposed scheme for the reason that there are considerable errors in manual measurements due to various approximate operations. The proposed bi-temporal TLS measurement scheme should be verified by comparing the volume measurements of bulk grains with the standard value that has been previously determined. This verification method can be used to determine the correctness and accuracy of the measurement scheme without considering the effect of geometrical deformation.

We conducted repeated TLS measurements 10 times at different sampling rates on a standard experimental granary bin with a known volume value. Figure 12 shows the standard bin's appearance and structure. It belongs to a square steel silo with a regular shape and smooth surface, whose volume can be estimated according to standard geometric formula. Yet a high-precision total station with 5" for horizontal and angle accuracy and ±2mm + 2ppm×D for distance accuracy is utilized to obtain more accurate volume value for the standard bin. Setting out enough observed points can achieve 1‰ accuracy for the total station-based volume measurement, whose result is regarded as a reference value for correctness verification. The workflow described in Section 2 was applied to the TLS dataset acquired in the standard bin again. Volume calculation results at different sampling rates are listed in Table 4, in which the sampling rate - 1/*n* means that one data is taken every *n* rows/columns from the original TLS data. From Table 4, although the sampling rate has some effect on the accuracy of volume measurements, the correctness and repeatability of the proposed scheme were verified by 60 repeated test results.

Error analysis

The error data listed in Table 2 show that the average error between the TLS measurement and the artificial measurement is within 4%. The volume values calculated by the TLS-based 3D modeling are assumed to be closer to the true values. Table 4 reveals that there exist systematic errors in the measured results. Systematic errors are mainly caused by experimental errors, data acquisition errors and modeling errors. Generally, experimental errors could exist in the measurement procedure, instrument oper-

Table 2. Comparison of calculated volumes between the proposed 3D modeling-based scheme and the conventional manual measurement and calculation method.

TLS Dataset	Calculated Volume (m^3)		Relative error
	By 3D modeling	By manual measurement	
#1	3548.87	3545.32	0.1%
#2	5238.78	5222.29	0.3%
#3	764.23	773.41	1.2%
#4	2973.01	2919.48	1.8%
#5	1568.13	1604.25	2.3%
#6	1305.44	1258.64	3.7%
#7	819.15	847.82	3.4%
#8	1240.75	1272.06	2.5%

TLS, terrestrial laser scanning.

Table 3. Running time for each task of the proposed bi-temporal multi-site terrestrial laser scanning scheme for 3D modeling and volume measurement.

TLS Dataset	No. of sites	Loading condition	Average surv. time per site (sec.)	CPU running time (sec.) Preprocess	Registration	Others	Total (min.)
#2	4	Empty Full	184 178	48 40	288	74	31.63
#6	4	Empty High	193 189	56 48	316	81	33.82
#7	2	Empty Low	161 160	16 16	87	46	13.45

ation, environmental conditions, and so on. To eliminate systematic experimental errors, experimenters should be required good insight, proper tools and guidelines. This subsection focuses on the analysis of the latter two errors.

The data acquisition errors are reflected by the quality of TLS point cloud. Among the factors influencing the quality of point cloud data, the sampling rate is the most important one, which determines the resolution and density of a point cloud. Table 4 indicates that a low TLS sampling rate could induce considerable measurement errors. Although increasing the sampling rate can reduce the error, it will produce a large volume of data, which implies a high computational cost. A compromise should be reached between the computational efficiency and the measurement accuracy. Experimental results show that a sampling rate of 1/3 or 1/4 for the original TLS data can fully satisfy the ultimate accuracy requirements.

The modeling errors refer to miscellaneous errors generated in the TLS-based methodological workflow for 3D modeling and volume calculation of bulk grains. As the automatic markerless multi-site registration is a vital task in the entire mathematical processing, registration accuracy would directly affect the magnitude of modeling errors. The overall registration accuracy can be quantitatively assessed by a pair of error metrics widely adopted by the academic literature on point cloud registration: rotation error (RE) and translation error (TE). RE and TE evaluate the estimated pose against its ground truth by measuring the registration errors of features used for correspondence matching (Hu *et al.*, 2021). The proposed automatic marker-free registration method can achieve high geometrical accuracy of a maximum RE of 7° and a maximum TE of 5 cm by making the correspondence determination from routine to concrete, which is very helpful in reducing modeling errors to a very low level.

Conclusions

This paper presents a bi-temporal TLS scheme for fast 3D modeling and accurate volume measurement of bulk grains stored in large warehouses. The use of bi-temporal TLS data provides the scheme with the ability to capture complete surface information about a grain bulk and accurately reconstruct its 3D volumetric model accordingly. The scheme-specific methods or techniques, including automated marker-free multi-view registration, region growing-based surface extraction and triangular facet projection-based volume calculation, can accomplish reliable and fast model reconstruction and volume measurement by exploring the large grain storehouse's structural characteristics. Experimental results reveal that the proposed 3D modeling and volume measurement

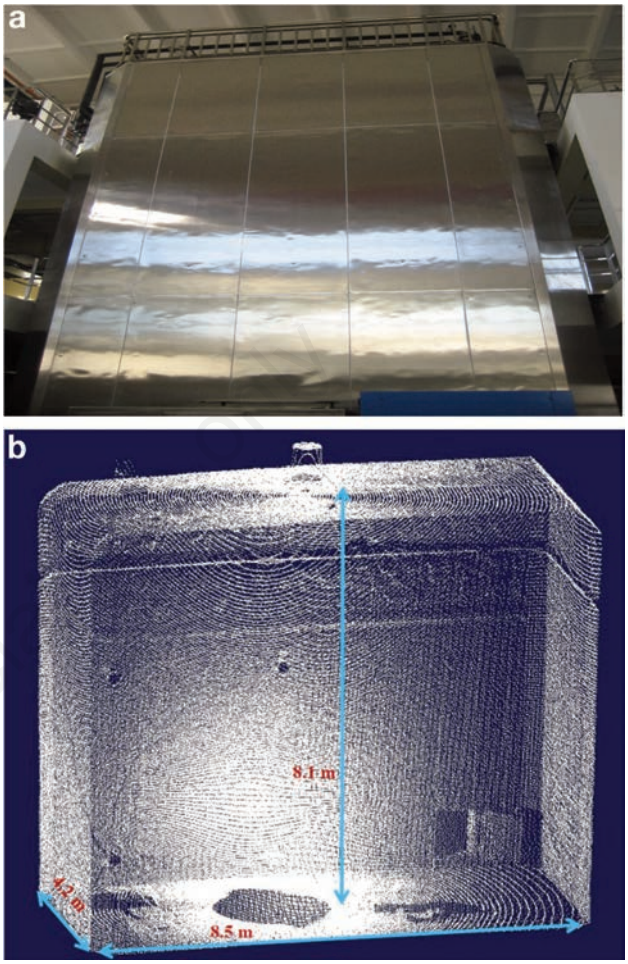

Figure 12. A standard granary bin for experimental verification. (**a**) Appearance; (**b**) structure.

Table 4. Measured values of the volume for a standard experimental granary bin with a known volume value of 229.57 m^3.

Sampling rate (1/n)	Volume values calculated for ten repeated tests (m^3)	Mean (m^3)	Standard devaition (m^3)	Relative error
1	228.55, 229.92, 230.52, 230.47, 229.26, 231.16, 229.67, 229.73, 229.30, 229.08	229.76	0.78	0.08%
1/2	230.57, 229.03, 229.91, 229.34, 230.09, 229.29, 230.26, 230.48, 231.34, 228.65	229.89	0.82	0.14%
1/3	228.37, 227.79, 226.95, 229.44, 229.16, 228.95, 227.16, 230.31, 229.24, 228.44	228.58	1.05	0.43%
1/4	228.45, 228.02, 225.89, 227.99, 227.19, 226.97, 226.71, 227.63, 225.97, 229.83	227.46	1.19	0.92%
1/5	224.89, 223.90, 223.42, 229.97, 228.28, 225.86, 223.62, 223.77, 225.36, 226.94	225.60	2.20	1.73%
1/6	222.38, 226.98, 223.39, 223.51, 226.18, 227.15, 222.85, 227.59, 226.39, 222.95	224.94	2.08	2.02%

scheme can work effectively and quickly in TLS-based granary field applications and repeated test data demonstrate its correctness, repeatability and accuracy. Compared with the conventional manual measurement approach, the bi-temporal TLS scheme can not only achieve much higher measurement precision, but also greatly improve efficiency by significantly reducing cost, workload, and manpower. Noteworthily, the proposed scheme is a dedicated solution for TLS-based measurement in rectangular grain storehouses. The major limitation of the scheme is that it is difficult to extend to other structured grain storehouse (*e.g.*, circular silos). Future work is still needed to develop a more generic TLS scheme for bulk grain measurement to enhance its potential for use in the area of national grain inventory inspection in China.

References

Barreca F., Modica G., Di Fazio S., Tirella V., Tripodi R., Fichera C.R. 2017. Improving building energy modelling by applying advanced 3D surveying techniques on agri-food facilities. J. Agric. Eng. 48:203-8.

Buckley S.J., Howell J.A., Enge H.D., Kurz T.H. 2008. Terrestrial laser scanning in geology: data acquisition, processing and accuracy considerations. J. Geol. Soc. 165:625-38.

Chen W., Hu X., Chen W., Hong Y., Yang M. 2018. Airborne lidar remote sensing for individual tree forest inventory using trunk detection-aided mean shift clustering techniques. Remote Sens. 10:1078.

Chen Y., Medioni G. 1992. Object modelling by registration of multiple range images. Image Vis. Comput. 10:145-55.

Hu X., Chen W., Xu W. 2017. Adaptive mean shift-based identication of individual trees using airbome lidar data. Remote Sens. 9:148.

Hu X., Yang L., Wu F., Tian Y. 2021. Robust markerless registration of point clouds for terrestrial laser scanning-based measurement of bulk grains stockpiled in storehouses. Appl. Eng. Agric. 37:1073-87.

Huising E.J., Pereira L.M.G. 1998. Errors and accuracy estimates of laser data acquired by various laser scanning systems for topographic applications. ISPRS J. Photogram. Remote Sens. 53:245-61.

Liang X.H., Sun W.D. 2011. A fast 3d surface reconstruction and volume estimation method for grain storage based on priori model. Proceedings of International Symposium on Photoelectronic Detection and Imaging, International Society for Optics and Photonics, Beijing. pp. 165-77.

Lumme J., Karjalainen M., Kaartinen H., Kukko A., Hyyppä J., Hyyppä H., Jaakkola A., Kleemola J. 2008. Terrestrial laser scanning of agricultural crops. Int. J. Remote Sens. 26:563-6.

Marton Z.C., Rusu R.B., Beetz M. 2009. On fast surface reconstruction methods for large and noisy point clouds. International Conference on Robotics and Automation (ICRA), IEEE, Kobe. pp. 3218-23.

Montuori A., Luzi G., Stramondo S., Casula G., Bignami C., Bonali E., Bianchi M.G., Crosetto M. 2014. Combined use of ground-based systems for cultural heritage conservation monitoring. Proceedings of IEEE Geoscience and Remote Sensing Symposium (IGARSS), IEEE, Quebec City. pp. 4086-9.

Nurunnabi A., Belton D., West G. 2012. Robust segmentation for multiple planar surface extraction in laser scanning 3d point cloud data. 21st International Conference on Pattern Recognition (ICPR), IEEE, Tsukuba. pp. 1367-70.

O'Neal M.A. 2014. Terrestrial laser scanner surveying in coastal settings, in: Finkl, C., Makowski, C. (Eds.), Remote Sensing and Modeling. Springer Int. Pub. 3:65-76.

Park G., Park K., Song B. 2021. Spatio-temporal change monitoring of outside manure piles using unmanned aerial vehicle images. Drones 5:1.

Pu S., Vosselman G. 2009. Knowledge based reconstruction of building models from terrestrial laser scanning data. ISPRS J. Photogram. Remote Sens. 64:575-84.

Ren Z. 2007. Practice of grain inventory checking. Beijing: China Commercial Publishing House.

Reshetyuk Y. 2009. Terrestrial laser scanning: error sources, self-calibration and direct georeferencing. VDM Verlag, Saarbrűcken. Rosin, P.L., 1999. Measuring rectangularity. Mach. Vis. Appl. 11:191-6.

Rusu R.B. 2009. Semantic 3D object maps for everyday manipulation in human living environments. Ph.D. thesis. Technische Universitaet Muenchen.

Rusu R.B., Cousins S. 2011. 3d is here: Point cloud library (pcl). Proceedings of the International Conference on Robotics and Automation (ICRA), IEEE, Shanghai. pp. 1-4.

Shao Q., Xu T., Tatsuo Y., Song N., Zhu H. 2016. Classified denoising method for laser point cloud data of stored grain bulk surface based on discrete wavelet threshold. Int. J. Agric. Biol. Eng. 9:123-31.

Wang Y., Wang J., Chen X., Chu T., Liu M., Yang T., 2018. Feature surface extraction and reconstruction from industrial components using multistep segmentation and optimization. Remote Sens. 10:1073.

Yon J., Cheng S.W., Cheong O., Vigneron A. 2017. Finding largest common point sets. Int. J. Comput. Geom. Appl. 27:177-85.

Zeng S.Z., Lin T.C., Tsou C.F., Lu S.H. 2012. The method for measuring the grain volume in large storage tank. J. Agri. Fore. 61:399-410.

Zhu T., Shi Y., Meng F., Hu T., Wang Y., Li E., Zheng G. 2012. Study on measuring grain bulk by laser scanning. Grain Sci. Technol. Econ. 37:30-1.